

The strength of frustration and quantum fluctuations in LiVCuO_4

SATOSHI NISHIMOTO¹, STEFAN-LUDWIG DRECHSLER^{1 (a)}, ROMAN KUZIAN^{1,2}, JOHANNES RICHTER³,
JIŘI MÁLEK^{1,5}, MIRIAM SCHMITT⁴, JEROEN VAN DEN BRINK¹, AND HELGE ROSNER⁴

¹ Leibniz-Institut für Festkörper- und Werkstoffforschung (IFW) Dresden, D-01171 Dresden, PF 270116, Germany

² Institute for Problems of Materials Science Krzhizhanovskogo 3, 03180 Kiev, Ukraine

³ Institut für Theoretische Physik, Universität Magdeburg, Magdeburg, Germany

⁴ Max-Planck-Institut für Chemische Physik fester Stoffe, Dresden, Germany

⁵ Institute of Physics, ASCR, Prague, Czech Republic

PACS 74.72.Jt – Other cuprates

PACS 78.70.Nx – Neutron inelastic scattering

PACS 75.30.Ds – Spin waves

Abstract –We present an empirical and microscopical analysis of the main in-chain exchange constants of the edge-shared frustrated chain cuprate $\text{LiVCuO}_4 = \text{LiCuVO}_4$ with a ferromagnetic nearest neighbour coupling which clearly exceeds the antiferromagnetic (AFM) next-nearest neighbour exchange J_2 . The measured saturation field is significantly affected by a weak 3D AFM interchain coupling leaving room for a possible Bose-Einstein condensation for several T below. The obtained exchange parameters are in agreement with the results for a realistic five-band extended HUBBARD Cu $3d$ O $2p$ model, LSDA+ U predictions as well as with inelastic neutron and magnetization data. The single chain frustration rate $\alpha = J_2/|J_1| \approx 0.75$, including all error bars, is definitely smaller than 1.0 which correspond to strongly coupled interpenetrating AFM Heisenberg chains in contrast with opposite statements in the literature. A proper account of strong quantum fluctuations and frustration is necessary for a correct assignment of the exchange integrals. which cannot be achieved by a simple renormalization of J_2 from spin-wave theory.

1. INTRODUCTION. – $\text{LiVCuO}_4 \equiv \text{LiCuVO}_4$ is one of the first [1,2] and rather frequently studied spin-chain compounds among edge-shared cuprates [3–7]. Recently it became especially interesting due to the observation of multiferroicity [8–10] and due to a possible realization of quantum spin nematics and related Bose-Einstein condensation of two-magnon bound states in high magnetic fields [11–13]. Both phenomena are still poorly understood and a precise knowledge of the main exchange interactions is of key importance to attack such complex problems in a realistic way. Unfortunately, there is no consensus about the magnitude of these couplings and in particular on the value of the in-chain frustration parameter $\alpha = J_2/|J_1|$, with $J_1 < 0$ as the ferromagnetic (FM) nearest neighbor (NN) and J_2 the antiferromagnetic (AFM) next-nearest neighbor (NNN)-coupling in chain direction b (see Fig. 1). So far, in various studies $0.5 \leq \alpha \leq 2.2$ and even above 5.5 have been predicted/reported. [3,5,14–16]

Keeping in mind the weak interchain coupling, the single-chain can be viewed also as two interacting and interpen-

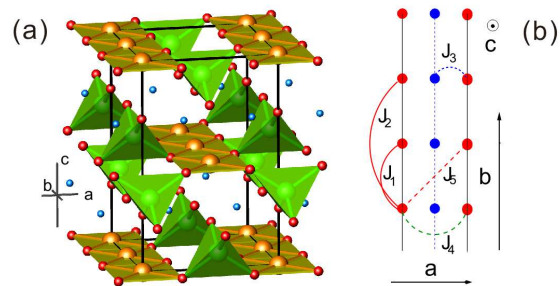


Figure 1: (Color) (a): the crystallographic structure of LiVCuO_4 comprises two AFM coupled CuO_2 spin-chains per unit cell running along the b -axis (orange \bullet – Cu^{2+} , red \bullet – O^{2-} , bright blue \bullet – Li^+). (b): the main in- and inter-chain exchange paths, J_1 , J_2 , and J_3, J_4, J_5 marked by solid red arcs, broken red line, blue and green arcs, respectively.

^(a)Corresponding author, E-mail: s.l.drechsler@ifw-dresden.de

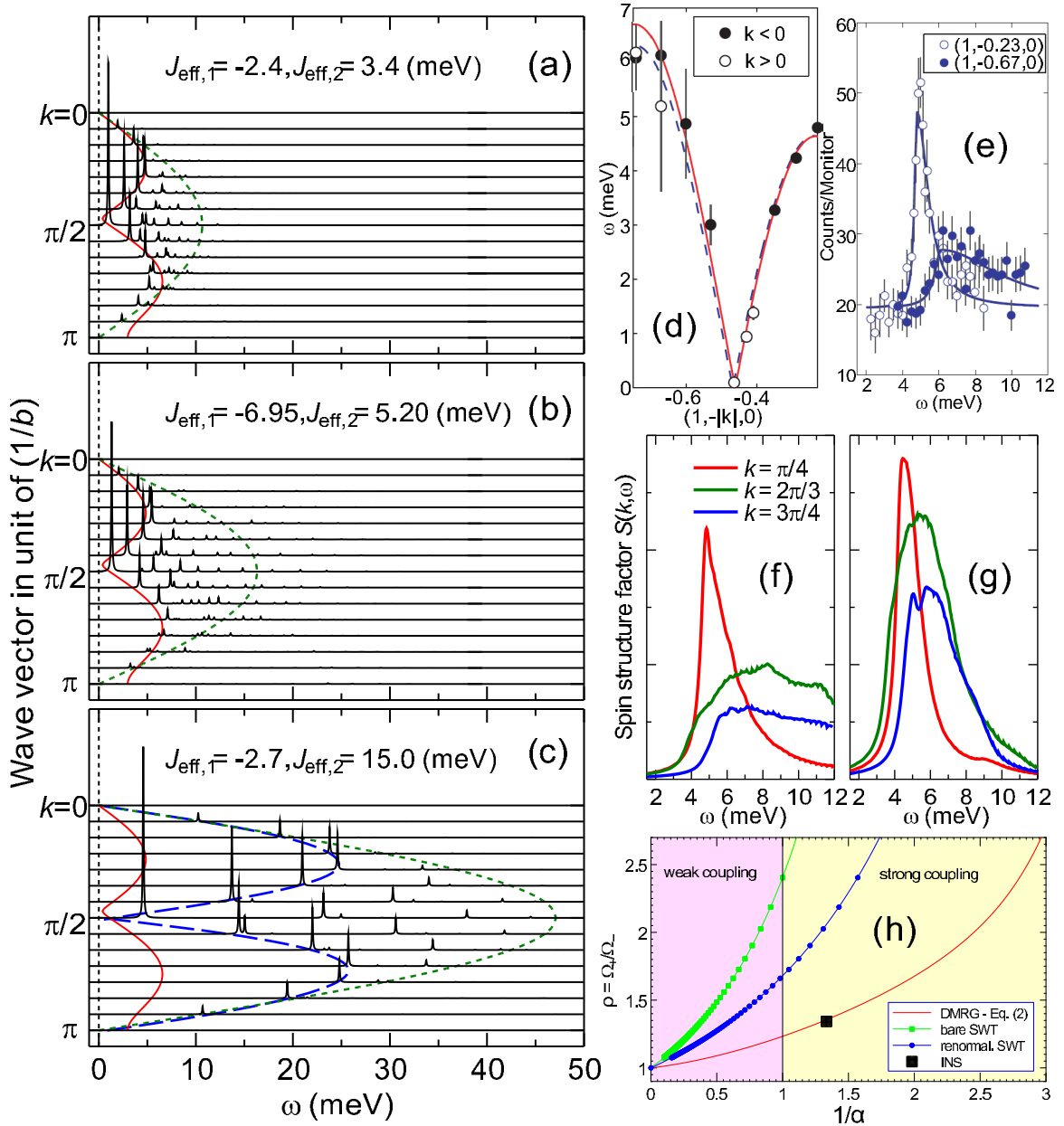


Figure 2: (Color) Left: Magnetic dynamical structure factor $S(k, \omega)$ from exact diagonalizations for periodic chains and $L = 28$ sites for the parameter sets proposed in Ref. [5] (a), our recent findings [16] (b) and that by Koo *et al.* [15] for $U = 5$ eV (see Tab. 1) (c). Right: experimental *asymmetric* dispersion along the chain direction in between Ω_+ and Ω_- (see Fig. 2(h) and Eq. (2)) and INS-intensities from Ref. [5] (d,e), calculated $S(k, \omega)$ normalized to the static structure factor $S(k)$ (i.e. the ω -integrated dynamical one) for a single chain with our parameters (f) and that of Ref. [5] (g), and the ratio of the peak positions at the first and second maximum of $S(k, \omega)$ for the transferred momenta near $k=1/4$ and $3/4$, respectively, (h) approximately given by the red curves in (a-c). In all DMRG-calculations for chains with open boundary conditions, $L = 96$ sites, and a Lorentzian broadening at half-width $\Gamma = 0.3$ meV have been employed.

etrating simple AFM Heisenberg chains (AHC) or equivalently as a single zigzag ladder. Then, one is left with a weak ($\alpha > 1$) or a strong coupling scenario in the opposite case $0 < \alpha < 1$ because $1/\alpha$ provides a direct measure of the FM "interchain"-coupling within a zigzag-ladder or between interpenetrating AHC. Here, we give a more comprehensive presentation of arguments *against*

weak coupling scenarios than in our short Comment [16] on Ref. [5] and rebut in more detail also arguments put forward in Ref. [6]. In addition, the striking discrepancy of a very recent parameter set obtained in Ref. [15] with available experimental data, including also Refs. [5, 6] will be shown, too. Finally, the reasons of the incorrect parameter assignment given in Refs. [3, 5, 15] are explained

Table 1: Exchange integrals (in meV) as extracted from INS data using bare spin wave theory (BSWT), ad hoc renormalized spin wave theory (RSWT) [3] or RPA [5] as compared with parameters derived from mapping of microscopic models (see sect. 3). In all LDA(GGA)+ U shown calculations a value $U - J = 5$ eV appropriate for edge-shared cuprates has been used.

| | J_1 | J_2 | α | J_4 | J_5 |
|---------------|-------|-------|----------|-------|-------|
| BSWT [3] | -1.6 | 5.59 | 3.49 | 0.01 | -0.4 |
| RSWT [3] | -1.6 | 3.56 | 2.23 | | |
| RPA [5] | -2.4 | 3.4 | 1.42 | | |
| present work | -6.95 | 5.2 | 0.75 | | |
| 3dO2p optics | -6.31 | 5.05 | 0.8 | | |
| GGA+ U [15] | -2.7 | 15.0 | 5.55 | -1.31 | 0.16 |
| LSDA+ U | -8.5 | 7.05 | 0.82 | | |
| GGA+ U | -6.4 | 5.45 | 0.85 | | |

in terms of an improper handling of strong quantum fluctuations (SQF). Clear evidence for SQF comes from the small values of the ordered magnetic moment of $0.31\mu_B$ and the low Néel-temperature $T_N \approx 2.4$ K [2, 10].

2. PHENOMENOLOGICAL ANALYSIS.

The low-energy inelastic neutron scattering (INS) data [3] have been fitted in terms of simple (bare) 3D spin wave theory (BSWT), i.e. *without* any renormalization or account of quantum fluctuations (see Figs. 2 (a-c,d,e)). As a result one arrives at $J_2^{\text{BSWT}} \approx 5.6$ meV and $J_1^{\text{BSWT}} \approx -1.6$ meV despite weak interchain couplings among them $J_5^{\text{BSWT}} = -0.4$ meV has been claimed to be the predominant interaction responsible for the in-phase ordering of spirals in the magnetically ordered state below T_N (see Tab. 1). Then based on these and recent high-energy data ($20 \text{ meV} > \omega > 0.5 \text{ meV}$ data) [5] analyzed by means of a random phase approximation (RPA) approach for the account of the coupling between the AHC, an effective 1D model has been proposed in Ref. [5]:

$$J_{\text{eff},2} \approx (2/\pi)J_2^{\text{SWT}} \quad \text{and} \quad J_{\text{eff},1} \approx J_1^{\text{SWT}} + 2J_5^{\text{SWT}}, \quad (1)$$

Thereby quantum fluctuations have been taken into account by the prefactor $2/\pi$ as for free AHC in accord with the implicate *a priori* assumption of a weak coupling between the AHC, in other words any renormalization related to the coupling $J_{\text{eff},1}$ between the AHC has been almost ignored. Such an assumption seems to be to not justified from a general many-body theory point of view. However, following our recent work [16] we will show here in more detail that the in-chain exchange integrals J_1 and J_2 , respectively, are significantly different from those suggested in Refs. [3, 5, 6, 15]. Furthermore it has been claimed that the FM coupling J_1 can be fixed at its bare value $J_1^{\text{BSWT}} = J_1^{\text{RSWT}}$. This would yield $J_2^{\text{RSWT}} \approx 3.57$ meV close to the result of a phenomenological RPA-based description of the problem: $J_2^{\text{RPA}} \approx 3.4$ meV [5]. In passing through we note that the value predicted by Koo *et al.*

[15] exceeds that value very much by a factor larger than three. If the interchain coupling is of less relevance for the "high-energy" physics, the claimed $2J_5 \approx -0.8$ meV should be *added* to $J_1^{\text{RPA}} = -2.4$ meV only for low-energy problems such as thermodynamics, i.e. relevant for the saturation field and the magnetization or the determination of the spiral's pitch angle. With such a more convincing empirical RPA affected renormalization one would already arrive at $\alpha = 1.063$ close to the strong coupling boarder line. Up to now all considerations were based on the assumption that the FM J_1 remains fixed. However, field-theory flow-equations based approaches [17] valid at $\alpha \gg 1$ point to strong coupling renormalizations. As a consequence, J_1 might change considerably and α is further scaled down. In fact, such a tendency would be compatible with our DMRG [18] results (see also below and Tab. 1): $J_{\text{eff},1} = -6.95$ meV, $J_{\text{eff},2} = 5.2$ eV, and $\alpha \approx 0.75$ [16]. If one adopts the BSWT-parameters as a reasonable starting point, our results should be interpreted as a strong *upward* renormalization of both $|J_1|$ and a moderate for J_2 , too,

Turning first to the low-energy INS-data [3], we start with the two extrema of a one magnon excitation Ω_- and Ω_+ , i.e. the peak positions near the transferred momenta $k = 1/4$ and $k = 3/4$. This is the lowest two-spinon excitation (2SE) reproduced approximately by the BWST-fit taken from Ref. [3, 5]. Its dispersion is sketched by the red curves in Fig. 2 (a-c). Although the maximum corresponding to Ω_+ is broad, the asymmetry with respect to Ω_- quantified by the dynamical asymmetry parameter $\rho = \Omega_+/\Omega_- \geq 1$ is clearly visible in the INS-data in contrast with the set proposed in Ref. [15] where $\rho \approx 1$ would occur. On absolute scale a discrepancy by factor exceeding three between the experimental and the predicted dispersion is observed (see Fig 2(c) which can be traced back to artificially large values of J_2 (see Tab. 1).

From the experiment, Fig. 2 (d), one reads off $\Omega_- = 4.84$ meV. Taking $\Omega_+ = 6.4$ meV one estimates $\rho \approx 1.32$. ρ can be obtained from fitting our dynamical DMRG [19] results for $0.3 \leq \alpha \leq 3$ and long chains with $L = 96$ sites

$$\begin{aligned} \frac{\Omega_+}{J_2} &= \frac{\pi}{2} + 0.0338x - 0.302x^2 + 0.0831x^3 - 0.00699x^4, \\ \frac{\Omega_-}{J_2} &= \frac{\pi}{2} - 0.143x - 0.534x^2 + 0.279x^3 - 0.0589x^4 + \\ &\quad + 0.00465x^5, \end{aligned} \quad (2)$$

where the coupling strength $x = 1/\alpha = |J_1|/J_2$ has been introduced. The relation $\alpha = f(\rho)$ provides a convenient highly sensitive measure of the interaction regime which is heavily affected by the strong quantum fluctuations. The function $\alpha(\rho)$ is depicted in Fig. 2 (h). One realizes excellent agreement with $\alpha = 0.75$ derived in our previous paper where instead Ω_- and the relative magnetization curve $M(H)/M_s$ as a function of H/H_s at low temperature have been employed [16]. Notice the large deviations if the BSWT or the RSWT would be applied to extract α .

Taking $\Omega_+^{BSWT} \approx 6.7$ meV and $\Omega_-^{BSWT} \approx 4.75$ meV from Figs. 2 (d,e) which yields $\alpha^{BSWT} \approx 2.3$ almost consistent with 2.2 stated in Ref. [3]. Using the RPA-derived values one arrives at α^{RPA} about 1.42 again in formal consistency with [5]. The strong deviations of both values from our DMRG-based value clearly show the inapplicability of simple spin-wave theory based estimates. The physical reason is the incorrect treatment of strong quantum fluctuations in the title compound which manifest themselves also in a small magnetic moment as mentioned above and in relatively large pitch angles (see below).

Finally, considering briefly the calculated and the experimental INS intensities, at present only few comparisons are possible due to lacking publication of experimental spectra. Nevertheless, comparing e.g. the available data shown in Figs. 2 (d,e) one realizes that our set provides a better description of the intensity at large transferred momenta (Fig. 2(b)) as compared with that of Ref. [5]. A comparison of the theoretical shapes with more INS spectra would be helpful to reduce our error bars.

If one adopts that the experimental magnetization data up to the so-called field $H_{c3} \approx 40.5 \pm 0.2$ T ($H \parallel c$) where the peak in dM/dH occurs [12] is well-described by an effective 1D model, one arrives at the curves shown in Fig. 3. Notice the strong deviation of the weak-coupling proposal by Koo *et al.* [15]. Then, a dominant FM interchain coupling as proposed in Refs. [3,5] cannot be reconciled with these experimental data since for such a coupling the 3D saturation field is smaller than its 1D counterpart [20]. Also the spin susceptibility $\chi(T)$ is within an

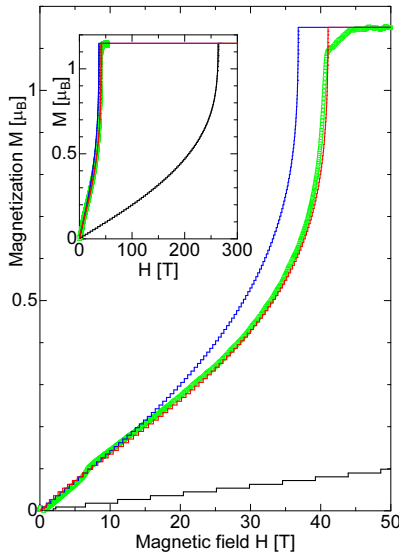


Figure 3: (Color) Magnetization vs. applied magnetic field. Experiment (\circ from Ref. [12]), theory: blue line - set of Ref. [5], red line - our set [16] and black line- the $U = 5$ eV- set from Ref. [15] and $g = 2.3$ for all sets. The DMRG calculations were performed for $L = 512$ sites at $T = 0$. Inset: 'entire' field range.

RPA approach for the interchain coupling best described by a total AFM interchain coupling. Anyhow, a detailed discussion of $\chi_s(T)$ including also a consideration of the background susceptibility χ_0 will be given elsewhere.

As mentioned above the presence of strong quantum fluctuations is evidenced by the small magnetic momentum of $0.31\mu_B$ and a low Néel-temperature $T_N = 2.4$ K. Both values should be compared e.g. with three to four times large values for the sister compound Li_2CuO_2 [21,22] caused by a relatively strong interchain coupling [23]. In addition its small $\alpha \approx 0.32$ is also helpful to suppress SQF. As a consequence the spiral state is significantly driven towards almost decoupled AHC the corresponding collinear Néel state, of each AHC i.e. the experimental pitch angle $\phi = 84^\circ$ analyzed within the BSWT or RSWT results in strongly overestimated α -values. This is illustrated in Figs. 4 and 5, where the maximum of the static magnetic structure factor is depicted as a function of α for the cases of a single frustrated J_1 - J_2 chain and a coupled pair of them, respectively. Already the latter is expected to provide a reasonable insight into the real quasi-1D situation. This point of view is supported by a detailed comparison with coupled cluster calculations to be reported elsewhere. Thus, for instance in the case of a planar arrangement of chains (i. e. a dominant 2D-interchain coupling as in the model adopted in Refs. [3,5,11,12]) the effective interchain interactions J_5^* and J_4^* correspond approximately to

$$J_5^* = 2J_5; \quad J_4^* = 2J_4 \quad . \quad (3)$$

Notice the striking failure of the classical curve especially

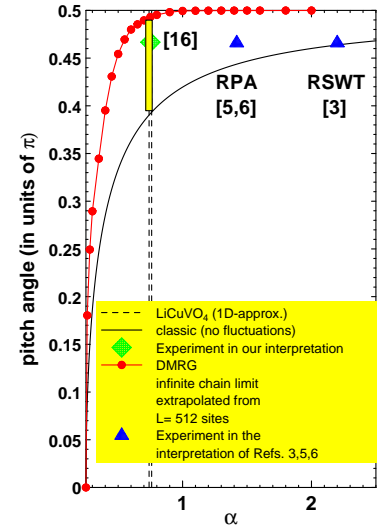


Figure 4: (Color) Pitch angle for a single chain from the maximum of the static magnetic structure factor $S(q)$ in comparison with experiment, Refs. [3,5,6], and Eq. (4) (black line).

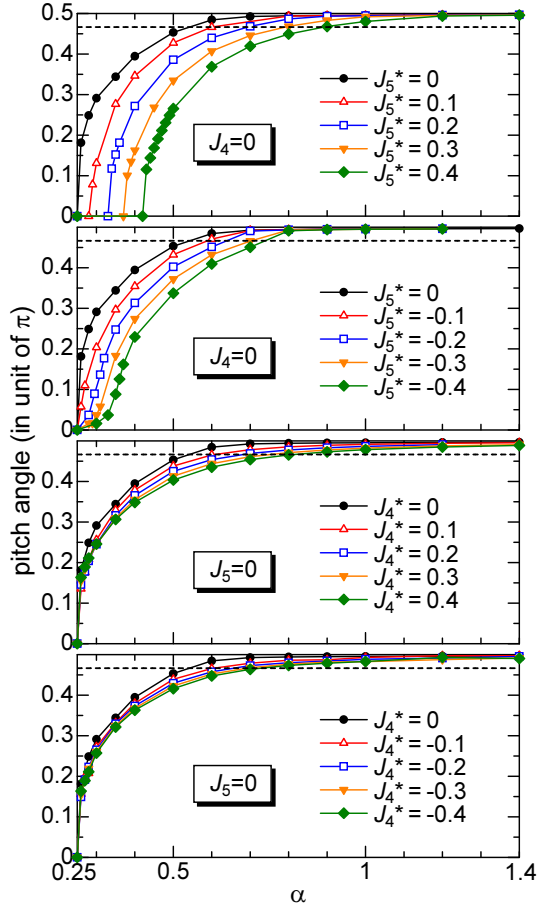


Figure 5: (color) Pitch angle for two coupled chains with various types of interchain coupling in units of $|J_1|$ (see Fig. 1(b)). The corresponding propagation vector has been estimated from the maximum of the calculated (DMRG) static magnetic structure factor $S(q)$ for $L = 192$ sites in total. The experimental value amounts about 0.467 (dashed line) [2].

for large α (see Fig. 4). Such an effect was first addressed in Ref. [24] in the 1D-case by means of DMRG and in Ref. [25] for a plane of perpendicularly coupled chains by means of a coupled cluster approach. We stress that the experimental value of the pitch [2] is reproduced for $\alpha \leq 1$, only, independently of the details of the weak interchain coupling. Adopting the in-chain parameters and the leading interchain coupling $J_5 \approx -0.4$ meV suggested in Ref. [3], one estimates from Fig. 5 a pitch angle of 89.58° ($\alpha = 2.22$) and of 89.43° in the case of the RPA derived set ($\alpha = 1.42$) in contrast to 84° known experimentally [2]. Thus, the measured ϕ points clearly to a strong coupling regime in contrast to opposite statements in Refs. [3, 5, 15]. Naturally, the SWT derived J 's obey nearly the classic relation, only, (i.e. completely ignoring the strong quantum fluctuations)

$$\phi = \cos^{-1}(0.25/\alpha), \quad (4)$$

yielding 83.53° for $\alpha = 2.22$ [3] (the small deviations from

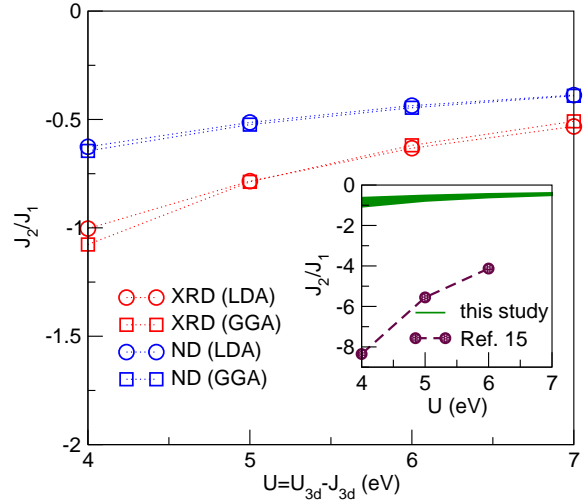


Figure 6: (Color) Frustration parameter α vs. effective on-site repulsion U for two different crystal structure refinements from x-ray (XRD) and neutron diffraction (ND). For each structure, two versions of the exchange correlation potential have been applied (LDA+ U and GGA+ U) within the around mean field double counting scheme and using $J_{3d} = 1$ eV. Inset: The range of the obtained α values from our calculations in dependence of U compared with the results of Koo *et al.* [15].

84° result from the weak interchain coupling ignored in Eq. (4) for the sake of simplicity) and 87.42° for $\alpha = 5.55$ [15]. What matters here is not the absolute value of ϕ , but the difference $\pi/2 - \phi$ which differs by two orders of magnitude between the quantum and the classic case [26]. Thus, the attempt to describe the spin dynamics in a quasi-classical way is the main reason for the improper assignment in Ref. [3].

3. MICROSCOPIC ANALYSIS. – Turning to a microscopic analysis, we compare our (DMRG) INS derived J 's with those from two independent microscopical approaches: (i) analyzing high-energy spectra from EELS, optical conductivity $\sigma(\omega)$ or RIXS data within strongly correlated extended multiband Hubbard models and a subsequent mapping of their spin-states onto the corresponding states of a spin-Hamiltonian, i.e. the 1D J_1 - J_2 model under consideration. The results are shown in Tab. 1 and Fig. 6. (ii) extracting these exchange parameters from total energy calculations of various prepared artificially magnetically ordered states (see e.g. [15]). A mapping from a Cu3d O2p five-band Hubbard model with usual parameters which describes the T -dependent dielectric response [27, 28] onto a J_1 - J_2 spin-1/2 model yields a sizeable $J_1 = -6.3$ meV and $J_2 = 5.05$ meV. We stress that in all closely related sister compounds [29] with a Cu-O-Cu bond angle $\lesssim 95^\circ$ sizeable FM $|J_1|$ -values $\gg 1.6$ meV have been found in fitting various data: Li₂CuO₂: $J_1 = -19.6$ meV (INS [23]), Ca₂Y₂Cu₅O₁₀: $J_1 = -14.7$ meV (INS [30]), Li₂ZrCuO₄: $J_1 = -23.7$ meV

($\chi(T)$, c_p [14,31]). In particular, also for LiVCuO₄ the T -dependent optical conductivity data [27] obtained from ellipsometry measurements can be well fitted within a five-band Cu 3d O 2p extended Hubbard model on chain-clusters with up to six CuO₄-plaquettes connected by edge-sharing. Thereby $U_d = 8$ eV, $U_p = 4.1$ eV $K_{pd} = 65$ meV, $\Delta_{pd} = 3.82$ eV etc. has been used. As a result one arrives at in-chain J 's close to the INS-derived ones: $\alpha = 0.8$ and $J_2 = 5.1$ meV (see Tab. 1). The value of J_1 is sensitive to the magnitude of the direct FM exchange K_{pd} whereas J_2 is mainly sensitive to the in-chain O-O transfer integrals. Thereby $|J_1| \propto K_{pd}$ holds approximately. Notice that the contribution of K_{pd} is much more important for the large negative (FM) value of J_1 than that of the intra-atomic FM Hund's rule coupling on O. In the past K_{pd} has been used mostly as a fitting parameter ranging from 50 to 110 meV for CuGeO₃ [32,33]. A reliable J_1 -value derived from an INS analysis as reported here is helpful to restrict its value and opens a door for systematic studies of this important exchange and useful comparisons with other sister compounds [29]. In fact, our empirical value corresponds to 130 meV for a σ -Cu-O bond to be compared with 180 meV estimated for that case and a cuprate plane in high- T_c superconductors [34].

Considering the total energies of various magnetic states the main exchange integrals can be also extracted from LDA+ U or GGA+ U calculations. Thereby the results depend mainly on a single parameter $U = U_{3d} - J_{3d}$, where $J_{3d} \approx 1$ eV denotes the Hund's rule coupling that is rather precisely known for transition metals. For both approximations, we calculated the exchange integrals J_1 and J_2 and their ratio α for the two different crystal structures refined from x-ray diffraction and neutron diffraction (labeled XRD and NRD, respectively, in Fig. 6 and below). As the key parameter, the resulting α for different values of U is presented in Fig. 6 and given in Table 1 ($U = 5$ eV). The graph indicates only small differences for the two crystal structure solutions, but essentially no difference for the two choices of the exchange-correlation potential (LDA+ U vs. GGA+ U). For realistic parameters which describe successfully other edge-shared chain cuprates one arrives again at $\alpha < 1$ in sharp contrast to Koo *et al.* [15] who obtained unusually large J_2 - and α -values not compatible with the observed pitch angle [2], the restricted two-spinon continuum, and an obviously *asymmetric* INS spectrum [5]. Presumably it is a consequence of the double counting procedure employed in Ref. [15] and *not* an artifact of the GGA as stated there because our calculations shown in Fig. 6 yield close values in the α -region of interest, both for the LDA and the GGA. Also the RPA-derived value $\alpha^{\text{RPA}} \sim 1.4$ [5] could be approached for unrealistic small U -values below 3 eV adopting the XRD data, only.

4. SUMMARY. – The main result of our revisited analysis of LiVCuO₄ is the clear evidence for *strong* coupling of AHC as derived from four independent experimental and theoretical studies: the INS yields a dynamical

asymmetry parameter ρ and a pitch angle very sensitive to quantum fluctuations. Weak coupling would result in a nearly collinear incommensurate state and in almost vanishing dynamical anisotropy, i.e. $\rho \rightarrow 1$ not compatible with the diffraction and INS data. The obtained values for the main exchange integrals are supported by independent microscopic calculations based on the L(S)DA+ U approach and the multiband Hubbard model.

We thank the DFG [grant DR269/3-1 (S.-L.D. & J.M.) and the Emmy-Noether-program (H.R.)], the programs PICS [contracts CNRS 4767, NASU 243 (R.O.K)], and ASCR(AVOZ10100520) (J.M.) for financial support.

References

- [1] HOPPE R., *et al.* *Z. anorg. allg. Chem.*, **379** (1970) 157
- [2] GIBSON B.J., *et al.* *Physica B*, **359** (2004) e253.
- [3] ENDERLE M., *et al.*, *Europhys. Lett.*, **70** (2005) 337
- [4] BUTTGEN N., *et al.* *Phys. Rev. B*, **81** (2010) 052403
- [5] ENDERLE M., *et al.*, *Phys. Rev. Lett.*, **104** (2010) 237207
- [6] ENDERLE M., *et al.*, *Phys. Rev. Lett.*, **106** (2011) in press
- [7] DRECHSLER S.-L., *et al.* *J. Phys. Condensed Matter*, **19** (2007) 145230
- [8] YASUI Y., *et al.*, *J. Phys. Soc. Jpn.*, **77** (2008) 023712
- [9] MOSKVIN A.S., *et al.* *EPL*, **81** (2008) 57004
- [10] SATO M., *et al.*; *Sol. State Sciences*, **12** (2010) 670
- [11] ZHITOMIRSKY M. AND TSUNETSUKO H., *EPL*, **92** (2010) 3701
- [12] SVISTOV L.E., *et al.*, *Pis'ma JETP*, **93** (2011) 24
- [13] DRECHSLER S.-L., *et al.*, *J. Mag. Mag. Mat.*, **316** (2007) 306
- [14] SIRKER J., *Phys. Rev. B*, **81** (2010) 024401
- [15] KOO H.-J., LEE C., WHANGBO M.-H., MCINTYRE G.J., and KREMER R.K., *Inorg. Chem.*, **50** (2011) 3582
- [16] DRECHSLER S.-L., NISHIMOTO S., KUZIAN R.O., J. MÁLEK, LORENZ W., *et al.*, *Phys. Rev. Lett.*, **106** (2011) in press
- [17] NERSESYAN A.A., *et al.*, *ibid.*, **81** (1999) 910
- [18] WHITE S.R., *ibid.*, **69** (1992) 2863
- [19] JECKELMANN E., *Phys. Rev. B*, **66** (2002) 045114
- [20] KUZIAN R.O. AND DRECHSLER S.-L., *ibid.*, **75** (2007) 024401
- [21] CHUNG E.M.L., *et al.* *ibid.*, **68** (2003) 144410
- [22] SAPIÑA F., *et al.*, *Sol. State Comm.*, **74** (1990) 779
- [23] LORENZ W., *et al.* *EPL*, **88** (2009) 37002
- [24] BURSILL R., *et al.* *J. Phys. Cond. Mat.*, **7** (1995) 8605
- [25] ZINKE R., *et al.* *Phys. Rev. B*, **79** (2009) 094425
- [26] ALIGIA A.A., *et al.* *ibid.*, **41** (2000) 3259. Here for both AFM J_1 , J_2 , the similar case $\phi - \frac{\pi}{2}$ is considered in 1D.
- [27] MATIKS Y., HORSCH, P., KREMER R.K., *et al.* *Phys. Rev. Lett.*, **103** (2009) 187401
- [28] MÁLEK J., DRECHSLER S.-L., NITZSCHE U., *et al.* *Phys. Rev. B*, **78** (2008) 060508(R)
- [29] DRECHSLER S.-L., *et al.* *J. Mag. Magn. Mat.*, **290** (2005) 345
- [30] KUZIAN R.O., *et al.* *in preparation*, (2011)
- [31] DRECHSLER S.-L., *et al.*, *Phys. Rev. Lett.*, **98** (2007) 07202
- [32] MIZUNO Y., *et al.* *Phys. Rev. B*, **57** (1998) 5326

- [33] BRADEN M., *et al. ibid.* , **44** (1996) 1105
- [34] HYBERTSEN M.S., *et al.,ibid.*, **45** (1992) 10032

